PCCP

Accepted Manuscript

ROYAL SOCIETY OF CHEMISTRY

www.rsc.org/pccp

Cite this: DOI: 10.1039/c0xx00000x

www.rsc.org/xxxxxx

ARTICLE TYPE

Molecular chemisorption on passivated and defective boron doped silicon surfaces: a "forced" dative bond

Khaoula Boukari,[a] Eric Duverger[b] and Philippe Sonnet*[a]

Received (in XXX, XXX) Xth XXXXXXXXX 20XX, Accepted Xth XXXXXXXXX 20XX

DOI: 10.1039/b000000x

We investigate the adsorption mechanism of a single trans 4-pyridylazobenzene molecule (denoted by PAB) on doped boron Si(111)√3x√3R30° surface (denoted by SiB) with or without boron-defect, by means of density functional theory calculations. The semiempirical approach proposed by Grimme allows us to take the dispersion correction into account. The role of the van der Waals correction on the adsorption geometries and energies is presented. In particular, two adsorption configurations are electronically studied. In the first one, the molecule is parallel to the surface and interacts with the SiB surface via the -N=N- bond. In presence of a boron-defect, a Si-N chemical bond between the molecule and the surface is then formed, while electrostatic or/and van der Waals interactions are observed in the defectless surface. In the second adsorption configuration, the molecule presents different orientations with respect to the surface and interacts via the nitrogen atom of the pyridyl part of the PAB molecule. If the molecule is perpendicular to the perfect SiB surface, the lone-pair electrons associated with the heterocyclic nitrogen atom fill the empty dangling bond of a silicon adatom via a dative bond. Finally, in presence of one boron-defect, the possibility of a "forced" dative bond, corresponding to a chemical bond formation between the PAB molecule and the silicon electron occupied dangling bond, is emphasized.

A. Introduction

The development of new semiconductor-based devices combining microelectronic technology with organic molecules is of high interest in many technological applications such as molecular electronics, sensors and materials for energy conversion [1-8]. In almost such cases, suitable substrates, particularly silicon based ones, allow to support the active molecules and hold them in place. However, in order to exploit their potential electronic properties, it is of crucial importance to understand the fundamental interactions between organic molecules and silicon based substrates [9-10]. In addition, as a result of the adsorption process, the molecule–silicon surface interactions may induce richer conformational changes than configurations observed in the phase gas or upon adsorption on metal surfaces.

The usual silicon surfaces (i.e. Si(001)2x1 and Si(111)7x7)) present a high density of reactive dangling bonds (DB's). The deposition of organic molecules on these surfaces leads to the formation of strong covalent bonds between the molecule and the substrate. The Si(111)√3x√3R30°-B (denoted by SiB) seems an ideal candidate to circumvent the problem of silicon reactivity with organic molecules. Indeed, due to the presence of boron atoms located in the S5 subsurface sites just below the silicon adatoms, the DB's of these adatoms are depopulated. In this position, the trivalent boron atoms, substituting silicon atoms, form four Si-B bonds. As a consequence, a charge is transferred from the DB's of the silicon adatoms to the boron atoms, leading to an empty DB's state. The Si(111)√3x√3R30°-B surface is then passivated [11-14].

A number of possible applications concerning molecular deposition on the SiB surface have been realized. For instance, the non destructive adsorption of different molecules on SiB surfaces at room temperature has been investigated by means of STM [15] and, seldom, DFT techniques [16-19]. These theoretical studies have shown that, despite non covalent interactions between molecule and silicon adatoms, the conformational shape of the molecule can be affected [15-19].

In the case of the trans 4-pyridylazobenzene molecule (denoted by PAB molecule and presented Figure 1) adsorption on the SiB surface, experimentally studied in reference 19, the authors have shown that the molecule is deposited on the surface but also in addition, that a reversible conformational switching (by means of scanning tunnelling microscopy (STM) via a pulse voltage at +3 V) is possible. This switching has been interpreted as a 180° rotation of the azophenyl moiety along a C-N bond. However no experimental observation allows to understand the interaction between the molecule and the SiB surface and, to our knowledge, no theoretical study has been carried out on this system. The authors only assumed that, thanks to the depopulated DB of the silicon adatom located above the boron defect, the molecule interacts with the SiB surface via the lone-pair electrons of the nitrogen atom located on the pyridyl part of the PAB molecule.

Indeed, the 4-pyridylazobenzene molecule is formed by a pyridyl part (i.e. pyridine molecule) and an azobenzene part (i.e. azobenzene molecule) linked by a covalent bond (Figure 1). The azobenzene and pyridine molecules and their derivatives have been intensively studied, experimentally as well as theoretically. The cases in which these molecules are deposited on different substrates were particularly investigated [20-50]. For instance, in reference 32, the pyridine adsorption on Cu(110) and Ag(110) surfaces has been studied in the framework of the DFT-D method using the semiempirical approach proposed by Grimme [51-55]. The pyridine molecule presents a nonbonding lone-pair of electrons localized on the nitrogen atom of the heterocycle. The authors have shown that the pyridine molecule interacts with the substrate and binds through the lone-pair electrons when its plane

is perpendicular to the surface or through the π electron system when its plane is parallel to the surface. These two possibilities are referred as N-bonding and π-bonding respectively. Intermediate cases, in which the molecular plane is tilted with respect to the surface, are also possible. On the other hand, E. McNellis *et al.* showed, by means of DFT calculations, that the azobenzene molecule adsorption on Cu(111), Ag(111) and Au(111) results from a competition between the covalent bonding of the central azo bridge (-N=N-) and the two closed-shell phenyl rings [43].

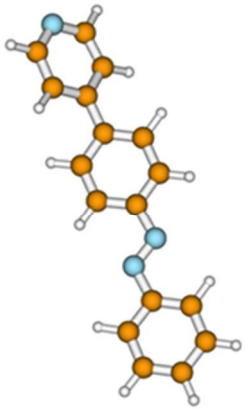

Figure 1 Ball-and-stick representation of 4-pyridylazobenzene molecule (denoted PAB) in a trans configuration. Orange, blue and white balls correspond to carbon, nitrogen and hydrogen atoms respectively.

However, the interaction of the 4-pyridylazobenzene molecule with the SiB substrate is not really known. For this reason, we present herein a DFT-D3 study of the isolated PAB adsorption on perfect and boron-defect SiB surfaces by envisioning different conformations. In order to evaluate the effect of the van der Waals interactions, energetic and structural calculations have been performed using the recent semiempirical approach proposed by Grimme [54-55]. While we note that the study in function of the concentration of the PAB adsorption will be particularly interesting, it is beyond the scope of this present work.

Finally, an electronic study has been realized (DOS (density of states), HOMO (high occupied molecular orbital) – LUMO (low unoccupied molecular orbital) charge density, electron function localization or ELF function) to analyze the specific molecule-substrate interactions.

B. Computational method and model

The calculations are performed in the framework of the density functional theory (DFT) implemented in the Vienna Ab-initio Simulation Package (VASP) [56-57]. Projector Augmented Wave (PAW) method, developed by Blöchl, were used to describe the electron-ion interaction [58-59]. The generalized gradient approximation (GGA) is used within the Perdew, Burke and Ernzerhof (PBE) exchange-correlation functional [60]. The cut-off energy for plane-wave is equal to 400 eV corresponding to carbon atom one. Due to the large unit cell used in our calculations (26.8 Å x 26.8 Å x 34 Å), the Brillouin zone integration is reduced to the Γ point. Increasing the number of k-point (from 1 to 4 irreducible k-points) does not modify the adsorption energy more than 0.02 eV. Furthermore, the adsorption energy considering spin polarized does not vary more than 0.03 eV with respect to no spin polarized simulations. In order to consider the dispersive interactions missing in the current DFT calculations, we use the DFT-D3 approach. Within the framework of the D3 correction the dispersion energy is the sum of two-body and three-body terms. The D3 correction is an approach based on an ab initio calculation of the C6 coefficients [54-55].

The Si(111)√3x√3R30°-boron, denoted by SiB, is modelled by periodic slabs containing four layers and one silicon adatoms layer. Hydrogen atoms saturate the backside of the slab. The hydrogen atoms are used in order to saturate and eliminate the dangling bonds states of atoms underneath the slab. This method allows to mimic a semi-infinite silicon crystal. The total number of atoms is 289. In the geometry optimization phase, the molecule, the adatoms layer and the three top most layers are allowed to relax while the last silicon and hydrogen layers are kept frozen. This model has been already used successfully in previous papers [18, 19]. The molecular and surface atomic structures are considered to be in equilibrium when the Hellmann Feynman forces are smaller than 0.02 eV/Å. The charge transfer occurring between the PAB and the surface were analyzed through a partial charges approach (i.e. valence electrons) in the Bader scheme [62-63].

In order to highlight the interaction between the PAB molecule and the SiB surface, electron localization function (i.e. ELF) representation has been used [64-66]. ELF is based on the Hartree-Fock pair probability of parallel spin electrons and can be calculated in density functional theory from the excess kinetic energy density due to Pauli-repulsion [67-68]. This function produces easily understandable, pictorially informative patterns of chemical bonding and is widely used to describe and visualize chemical bonding in molecules and solids [69]. The ELF is a measure of the probability of finding an electron near another electron with the same spin related to the Pauli Exclusion Principle [70-71].

C. Results

1.The Si(111)√3x√3R30°-Boron substrate: electronic structure

In the SiB substrate, silicon atoms are substituted by boron atoms in the third atomic layer directly below the silicon adatoms. A charge transfer occurs from the dangling bonds of the adatoms to the boron atoms. Thus, the top silicon adatoms present depopulated dangling bonds and the surface is passivated. The calculated density of states (DOS) of the perfect SiB surface is presented in figure 2a. The Fermi level is 0 eV and the calculated energy gap (1.05 eV) is in agreement with the experimental value (~1.3 eV) obtained by scanning tunneling spectroscopy (STS) at 5K [72].

However, the presence of boron-defects (i.e. the absence of boron atom below one adatom) is often observed by STM [19, 72]. We therefore consider in our calculations the possibility that the substrate presents one boron-defect. In this case, one boron atom is substituted by one silicon atom and the DB of the adatom located just above the boron defect is not passivated. Figure 2b shows the DOS of the SiB substrate involving one boron defect.

The peak at 0 eV, localized in the energy gap of the perfect SiB surface, corresponds to no depopulated dangling bond of the silicon adatom located above the boron defect. We can expect that the chemical reactivity of this dangling bond state is higher than those of the other silicon adatoms.

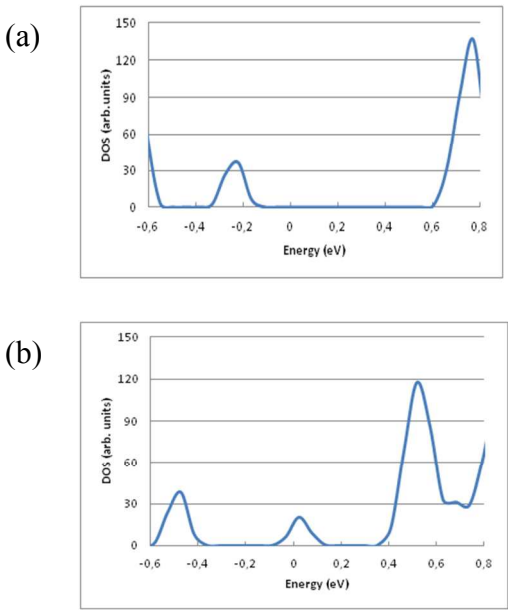

Figure 2 Density of states (DOS in arbitrary unit) of the perfect boron silicon surface (a) and of the one boron-defect silicon surface (b). The energy equal to 0 indicates the position of the Fermi level (E_F).

2.The 4-pyridylazobenzene molecule in gas phase: electronic structure

The atomic structure of the molecule is presented in Figure 1. The DOS of the free molecule (Figure 3a) shows the presence of two peaks at E_F-0.4 eV and E_F+1.4 eV corresponding to the HOMO and LUMO states respectively. The calculated gap of the PAB molecule is then 1.8 eV (energy between HOMO and LUMO peaks). The charge density maps of the HOMO and LUMO of the molecule in the gas phase are shown in Figures 3b and 3c. In the LUMO and HOMO, the stronger isodensity is located in the -N=N- bond of the azobenzene part of the molecule. In the pyridine part, the main contribution is located around the N atom. The LUMO and HOMO charge density maps are in good agreement with frontier orbitals of the pyridine [32] and trans-azobenzene [43] previously calculated.

Considering the charge density maps of the 4-pyridylazobenzene and taking into account the results of different papers [19-40], we can assume that the PAB molecule adsorbs without dissociation on the SiB surface via the –N=N- bond of the azobenzene part or via the N atom of the pyridyl one. In the following, we consider different cases in which the molecular plane is parallel, tilted or perpendicular with respect to the surface. In agreement with reference 19, we only study the trans molecular conformation (Figure 1).

3.Adsorption of the PAB molecule on SiB surfaces: energetic study

Two substrates have been considered: one presenting a perfect surface and the other a boron vacancy as observed experimentally [19, 72].

The adsorption energy of a given configuration is defined as:

$E_{ads} = E_{tot} – E_{isolated} - E_{substrate}$

where E_{tot} represents the total energy of the relaxed molecule/SiB surface system, $E_{isolated}$ is the energy of the relaxed PAB molecule in gas phase and $E_{susbtrate}$ is the energy of the relaxed clean SiB surfaces.

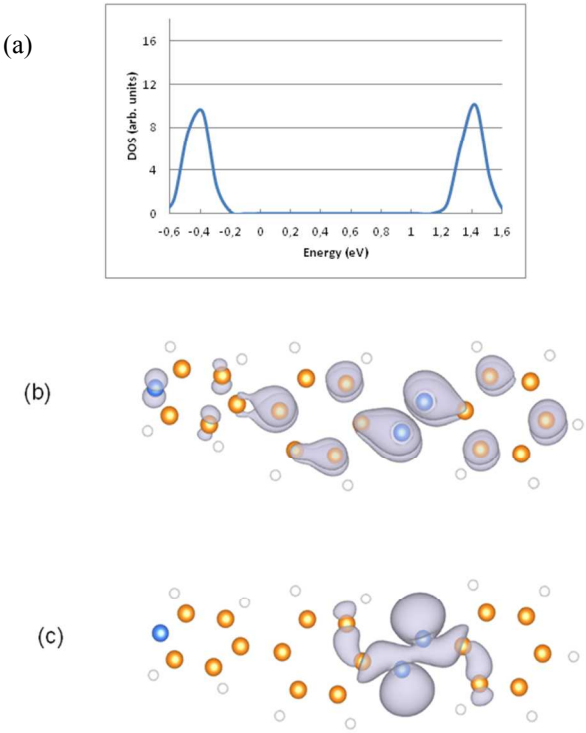

Figure 3 (a) Density of states (DOS in arbitrary unit) of the PAB molecule. The peaks at -0.4 eV and +1.4 eV correspond to the HOMO and LUMO states. (b) Isodensity map of the local density of states (LDOS) of the PAB molecule integrated between +1.34 eV and +1.49 eV corresponding to the LUMO states (isodensity = 0.02 e-/Å^3). (c) Isodensity map of the local density of states (LDOS) of the PAB molecule integrated between -0.36 eV and -0.56 eV corresponding to the HOMO states (isodensity = 0.02 e-/Å^3). The blue, orange and white balls correspond to nitrogen, carbon and hydrogen atoms respectively.

3a.Energetic study without the van de Waals correction

Eight possible adsorption configurations of the 4-pyridylazobenzene molecule on the SiB surface are investigated. These eight models are shown in Figure 4. In each case, a substrate with or without boron-defect is considered.

-Models M1 and M1d: PAB adsorption on one Si adatom parallel to the SiB substrate, via the -N=N- double bond, without and with boron vacancy respectively.

-Models M2 and M2d: PAB adsorption on one Si adatom parallel to the SiB substrate, via the N atom of the pyridyl part, without and with vacancy respectively.

-Models M3 and M3d: PAB adsorption on one Si adatom via the N atom of the pyridyl part in the tilted position, without and with boron vacancy respectively.

-Models M4 and M4d: PAB adsorption on one Si adatom via the N atom of the pyridyl part in the perpendicular position, without and with boron vacancy respectively.

We can note that increasing the number of silicon layers (up to eight silicon layers) does not vary the adsorption energy difference between the models M1 and M1d and between the models M4 and M4d more than 0.02 eV and 0.03 eV respectively.

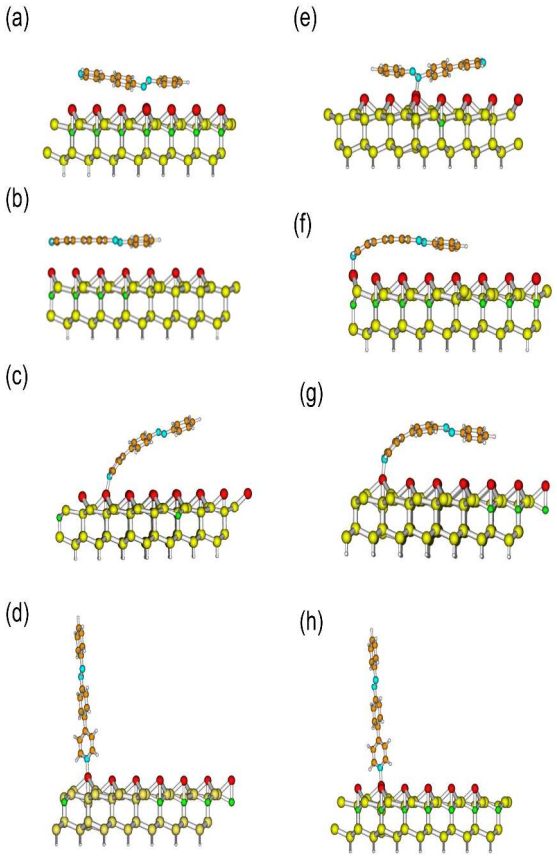

Figure 4 Side views of the optimized configurations of the eight models investigated in this work: (a) M1, (b) M2, (c) M3 (d) M4 (e) M1d (f) M2d (g) M3d (h) M4d. The d letter corresponds to boron defect surfaces. Red, yellow, green, blue, orange and white balls correspond to silicon adatoms, silicon, boron nitrogen, carbon and hydrogen atoms respectively.

The calculated adsorption energies and Si-N distances for the eight models are presented in Table 1.

Models	Eads (eV)	Si-N distance (Å)	Models	Eads (eV)	Si-N distance (Å)
M1	-0.14	2.28	M1d	-0.74	1.87
M2	-0.01	3.08	M2d	-0.51	1.86
M3	-0.38	1.98	M3d	-0.48	1.84
M4	-0.65	2.00	M4d	-0.88	1.85

Table 1 Adsorption energy (i.e. GGA approximation) and distance between the Si adatom and one of the N atoms of the 4-pyridylazobenzene molecule, for the Mn and Mnd models (with n varying from 1 to 4) shown in Figure 4.

The less stable models are M1 and M2 associated with the higher Si-N distances. In model M3, the tilted angle between the pyridyl part of the molecule and the surface destabilizes the adsorption energy with respect to model M4. The most stable model is M4 in which the molecule is perpendicular to the surface. In agreement with different authors [32, 40], the nitrogen lone-pair electrons of the pyridyl part of the PAB molecule interacts with the Si adatom in models M2, M3 and M4. This interaction is more effective when the molecule is perpendicular to the surface (M4 model) and, to a lesser extent, tilted (M3 model). M1 and M4 models are the most stable ones in agreement with theoretical results obtained for the pyridine molecule adsorbed on Cu(110) and Ag(110) surfaces [32, 40].

Concerning the M1d, M2d, M3d and M4d models, we notice that the boron defect stabilizes the four models. The models M2d and M3d present an adsorption energy similar despite different adsorption configurations. The most favourable ones are M4d and M1d models with the adsorption energies closer than those obtained in the perfect surface case. The Si-N distance, around 1.84-1.87 Å, is compatible with the formation of a chemical bond.

3b.Energetic study including the van de Waals correction

In a second step, we take the van der Waals correction into account as suggested by Grimme [51-55]. The adsorption energies and Si-N distances are reported in Table 2.

Taking the Grimme's term into account leads to the stabilization of all models. However, it favours more the parallel positions than the perpendicular ones, in agreement with the DFT studies concerning molecular adsorption on metallic surfaces [32, 41, 43]. Indeed, the Grimme's term is additive and thus when the molecule is in M1, M2 or, to a lesser extent, M3 positions, the number of atoms interacting with the surface increases strongly with respect to the perpendicular position (M4). Models M2 and M3, presenting both adsorption via the lone-pair electrons and parallel or tilted molecular position with respect to the surface, are energetically less likely than model M4. The adsorptions via the -N=N- bond (model M1) or the lone-pair (model M4) are now energetically very close.

Models	Eads (eV)	Si-N distance (Å)	Models	Eads (eV)	Si-N distance (Å)
M1	-0.93	2.32	M1d	-1.54	1.87
M2	-0.61	3.08	M2d	-1.18	1.83
M3	-0.69	2.00	M3d	-0.90	1.85
M4	-0.88	2.16	M4d	-1.13	1.86

Table 2 Adsorption energy (GGA + van der Waals approximation D3) and distance between the Si adatom and one of the N atoms of the 4-pyridylazobenzene molecule for the Mn and Mnd models (with n varying from 1 to 4) shown in Figure 4.

In presence of one boron-defect, the substrate reactivity is more important than in the perfect surface case. This stabilization may be due, in all cases, to a decrease of the molecule-substrate distance. The M1d model is largely more stable and the adsorption via -N=N- bond is therefore the most favourable mechanism. The M2d model, in which the molecule is parallel to the surface, is now more favourable than M3d and M4d models in which the molecule is tilted or perpendicular to the surface. In model M2d, all the atoms of the molecule are now closer to the surface than those of models M3d or M4d, favouring the van der Waals interactions and an important deformation of the molecule's pyridyl part. Following the perfect surface energetic study, the interaction of the nitrogen lone-pair electrons should be more efficient in the case of model M4d than in the M2d and M3d cases. One therefore can conclude that the energetic stabilization in the models M2d, M3d and M4d is a balance between the nitrogen lone-pair electrons interaction and the van der Waals one.

All our theoretical results highlight that the presence of one boron-defect in the substrate favours the molecular adsorption with respect to the perfect case. We suggest that, due to the presence of one charge in the dangling bond of the defect surface, the adsorption mechanism should be different in the perfect and boron-defect substrates cases. In order to better understand the observed differences between the PAB molecule adsorptions on the different SiB surfaces and elucidate the involved molecule-substrate interactions types, we now turn to the electronic structure.

4.Electronic study: Bader analysis and Electron Localization Function

In the following, we focus our DFT-D3 study on M1/M1d and M4/M4d models which correspond to two different adsorption mechanisms: one model parallel to the surface with adsorption via the double -N=N- bond and one model perpendicular to the surface with adsorption via the N atom of the pyridyl part of the PAB molecule.

A question now arises: which is the nature of the molecule-surface interactions? To address this question, we investigate the charge transfer and the electron localisation function (ELF) between the molecule and the substrate [64-66]. The Bader analysis allows us to evaluate the charge transfer between the molecule and the substrate. In order to identify the nature of the molecule-substrate interaction, we calculate the ELF function (Figure 5). The ELF is represented as a contour plot in real space, where different contours correspond to numerical values ranging from 0.0 to 1.0. The upper limit η=1.0 corresponds to a perfect localization (i.e. chemical bonding) while the value η=0.5 corresponds to an electron-gas-like pair probability (i.e. no chemical bonding). Thus, high ELF values show that, at the considered position, the electrons are more localized than in a uniform electron gas at the same density [67-71]. We have chosen to show only the values of the ELF between 0.5 and 1 in order to produce clearer figures.

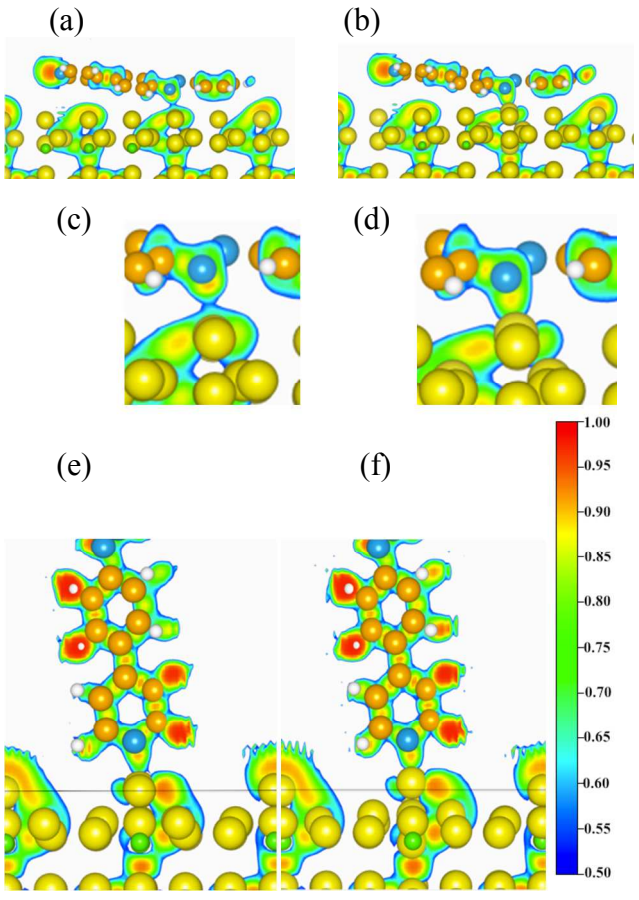

Figure 5 Side view of the electron localisation function (ELF) concerning models M1 (a), M1d (b), M4 (e) and M4d (f). (c) and (d) correspond to a zoom of the region between the PAB molecule and the substrate for the models M1 and M1d respectively. The d letter corresponds to boron defect surface. We have chosen to show only the values of the ELF between 0.5 and 1 in order to produce clearer figures. In right, the colour code of the ELF is the following: ELF=1.0 (in red) indicates an electron localized region, ELF=0.5 (in blue) corresponds to a delocalized region. The horizontal black line in the (e) and (f) emphasizes an atomic difference between M4 and M4d models: the adatom, which bonds with the molecule, is out of plane of the average position of the other adatoms (M4d model). Yellow, green, blue, orange and white balls correspond to silicon adatoms, silicon, boron, nitrogen, carbon and hydrogen atoms respectively.

Concerning model M1, a charge transfer of 0.06 e- occurs between the molecule and the surface. The distance between the molecule and the surface is 2.32 Å and is too large for a strong chemical bond. In Figure 5a and in the zoom of the Figure 5c, the blue boundary (η=0.5) in the region located between the -N=N- bond and the Si adatom indicates that there is no chemical bond between the molecule and the substrate. The nature of the molecule-substrate interaction is rather a van der Waals and electrostatic type interaction than a chemical bond. Energetically the van der Waals interaction is the major contribution (i.e. -0.79 eV) rather than the electrostatic one (i.e. -0.14 eV).

In the M1d model, the surface presents a boron-defect just below the -N=N- bond of the molecule and the charge transfer from the surface to the molecule is equal to 1.05 e-. The Si-N distance is 1.87 Å, in agreement with a possible chemical bond between the molecule and the substrate. In Figure 5b and in the zoom of the Figure 5d, the yellow region between the molecule and the substrate confirms the presence of a chemical bond. In order to form a bond with the Si adatom, the -N=N- double bond is broken.

In the M4 model, the charge transfer is 0.30 e-, directed from the surface to the molecule. The Si-N distance is 2.16 Å. In this case, the non-bonding electrons of the nitrogen atom of the pyridyl part interact with the empty dangling bond of the adatom. The ELF function shows the presence of a chemical bond between the molecule and the substrate (Figure 5e). Covalent bond occurs when electrons are shared by atoms in order to gain more stability. Dative bond occurs when one molecule donates both of the electrons needed to form a sort of covalent bond. In this case, the molecule serves as a donor and the substrate as an acceptor of electrons. Following our results, we propose that the bonding between the molecule and the substrate is dative. Indeed, the possible dative bonding on the silicon surface has already been proposed in previous papers. The chemical binding of the pyridine on the Si(001)2x1 surface has been studied by means of different spectroscopy methods and DFT calculations by Tao *et al* [73]. The Si(001) surface presents tilted Si-Si dimers. For instance, the bucking of the dimer is associated to the charge transfer from the buckled-down Si to the buckled-up Si. The Si-down presents an electron deficiency as well as the Si adatom of the SiB surface. The authors conclude that the pyridine molecules could interact with Si(001) through Si-down- lone-pair electrons of the N atom allowing a dative bonding. Furthermore, as presented by Zhang *et al* [74], the pyridine adsorption on the Si(111)7x7 surface have been studied by means of X-ray photoelectron spectroscopy and high-resolution electron energy spectroscopy. The authors showed the formation of a dative bond between the N-atom of pyridine and the corner adatom as well as the high thermal stability of this dative-bonded pyridine at room temperature.

Let us finally consider the M4d model. The charge transfer from the surface to the molecule is 0.68 e- and the Si-N distance is 1.86 Å. The ELF shows that models M4 and M4d exhibit an analogous adsorption mechanism (Figure 5f). Due to the position of the PAB molecule with respect to the surface, the molecule interacts with the Si adatom through the lone-pair electrons. However, in the boron defect case, the dangling bond is not empty. In this way, the formation of the Si-N bond should lead to a charge transfer from the substrate to the molecule. The Bader analysis shows that the silicon adatom, which binds with the nitrogen atom, loses 0.52 e- whereas, in the perfect case, this silicon adatom only loses 0.20 e-. This confirms the proposed adsorption mechanism that we denote by "forced" dative bond: the nitrogen lone-pair of electron interacts with the dangling bond of the Si adatom initially occupied by the charge resulting from the presence of a boron defect. The presence of the nitrogen lone-pair electrons forces a charge transfer from the adatom to the molecule.

D. Conclusions

We have realized a theoretical study of the adsorption of a single trans 4-pyridylazobenzene on boron doped Si(111)√3x√3R30° surfaces in the framework of the DFT-D calculations. In agreement with the experimental observations performed by STM, we have also considered the possible presence of a boron-defect on the SiB surface. Four models have been investigated: one adsorption via the -N=N- bond, the molecule being parallel to the surface, and three adsorptions via the N of the pyridyl part of the PAB molecule. This last mechanism occurs for three different angles with respect to the surface: parallel, at 45° and perpendicular. The energetic study shows that the presence of one boron-defect in the substrate favours the molecular adsorption with respect to the perfect case. The van der Waals correction stabilizes the parallel positions with respect to the perpendicular ones, in agreement with DFT studies concerning molecular adsorption on metallic surfaces [32, 41, 43]. Finally, the analysis of the charge transfer and the electron localization function (ELF) shows that when the molecule is parallel to the surface and adsorbed via the -N=N- bond, in presence of a boron-defect, a Si-N chemical bond between the molecule and the surface is formed. In the perfect substrate case, the interaction between the molecule and the surface is of electrostatic or van der Waals type.

In the case of adsorption via the N atom of the pyridyl part of the PAB molecule onto the perfect SiB surface, a dative bond occurs between the lone pair of the N atom and the empty Si adatom dangling bond. Previous study have already showed a dative bond formation between a pyridine molecule and different semiconductor surfaces as Si(001) [73], Si(111)7x7 [74] or Ge(100) [75]. In all cases, the authors have demonstrated that the pyridine molecules are dative-bonded to the electron-deficient silicon atoms of the surface. In our case, the presence of a boron-defect SiB surface, the dangling bond of the adatom located above the boron defect is now not empty. However, the orientation of the molecule and the ELF study show the same tendencies between the perfect and the boron-defect SiB surfaces. Due to the presence of the nitrogen lone pair electrons, a charge transfer is forced from the substrate (and particularly from the adatom) to the molecule. An unusual dative bond that we called "forced" dative bond is then established between the nitrogen atom and the electron rich silicon adatom dangling bond highlighted by a charge transfer from the adatom of the SiB surface to the molecule.

Finally, our theoretical study of the 4-pyridylazobenzene adsorption on SiB surfaces shows the rich interaction possibilities between a molecule and passivated and defective boron doped silicon surfaces.

Acknowledgments

This work was performed using HPC resources from GENCI-IDRIS (grant 2012-092042) and the supercomputer facilities of the Mésocentre de calcul de Franche-Comté. The French Agency ANR (ANR-09-NANO-038) has supported this work. We thank L. Stauffer for paper criticisms.

Notes and references

[a]*Institut de Science des Matériaux de Mulhouse (IS2M), CNRS UMR 7361, Université de Haute Alsace, 3b rue Alfred Werner 68093 Mulhouse cedex, France.* philippe.sonnet@uha.fr
[b]*Institut FEMTO-ST, Université de Franche-Comté, CNRS, ENSMM, 32 avenue de l'Observatoire, 25044 Besançon cedex, France.*

1 R. A. Wolkow, Annu. *Rev. Phys. Chem*. **50**, 413 (1999).
2 C. Joachim, J. K. Gimzewski, and A. Aviram, *Nature* (London) **408**, 541 (2000).
3 C. Joachim and M. A. Ratner, *Proc. Natl. Acad. Sci*. USA **102**, 8801 (2005).
4 V. Derycke, P. G. Soukiassian, F. Amy, Y. J. Chabal, M. D.D'Angelo, H. B. Enriquez, and M. G. Silly, *Nature Mater.* **2**, 253 (2003).
5 W. Yang, O. Auciello, J. E. Butler,W. Cai, J. A. Carlisle, J. E. Gerbi,D. M. Gruen, T. Knickerbocker, T. L. Lasseter, J. N. Russell, L. M. Smith, and R. J. Hamers, *Nature Mater*. **1**, 253 (2002).
6 W. Yang and R. J. Hamers, *Appl. Phys. Lett*. **85**, 3626 (2004).
7 J. Rubio-Retama, J. Hermando, B. López-Ruiz, A. Härtl,D. Steinmüller, M. Stutzmann, E. López-Cabarcos, and J. A. Garrido, *Langmuir* **22**, 5837 (2006).
8 A. Härtl, E. Schmich, J. A. Garrido, J. Hermando, S. C. R.Catharino, S. Walter, P. Feulner, A. Kromka, D. Steinmüller, and M. Stutzmann, *Nature Mater*. **3**, 736 (2004).
9 H. Yang, O. Boudrioua, A. Mayne, G. Comtet, G. Dujardin, Y. Kuk, Ph. Sonnet, L. Stauffer, S. Nagarajan, A. Gourdon, *Phys. Chem. Chem. Phys.* **14** ,1700 (2012).
10 O. Boudrioua, H Yang, Ph. Sonnet, L. Stauffer, A. Mayne, G. Comtet, G. Dujardin, Y. Kuk, S. Nagarajan, A. Gourdon, E. Duverger, *Phys. Rev. B* **85**, 035423 (2012).
11 P. Bedrossian, R. D. Meade, K. Mortensen, D. M.Chen, J. A. Golovchenko and D. Vanderbilt, *Phys. Rev. Lett*. **63**, 1257 (1989).
12 I.-W. Lyo,, E. Kaxiras, and Ph. Avouris, *Phys. Rev. Lett*. **63**, 1261 (1989).
13 E. Kaxiras, K. C. Pandey, F. J. Himpsel and R. M. Tromp, *Phys. Rev. B* **41**, 1262 (1990).
14 H. Shi, M.W. Radny and P.V. Smith, *Surf. Rev. and Lett*. **10**, 201 (2003).
15 M. El Garah, B. Baris, V. Luzet, F. Palmino and F. Chérioux, *ChemPhysChem* **11**, 2568 (2010).
16 M. El Garah, Y. Makoudi, F. Palmino, E. Duverger, Ph. Sonnet**,** L. Chaput, A. Gourdon and F. Cherioux, *ChemPhysChem* **10**, 3190 (2009).
17 B. Bulent, V. Luzet, E. Duverger, Ph. Sonnet, F. Palmino, F. Cherioux, *Angew. Chem. Inter. Ed*. **50**, 4094 (2011).
18 K**.** Boukari**,** Ph**.** Sonnet, E. Duverger, *ChemPhysChem* **13**, 3945 (2012).
19 K. Boukari, E. Duverger, Ph. Sonnet, *J. of Chem. Phys*. **138**, 084704 (2013).
20 M. El Garah, F. Palmino and F. Chérioux, *Langmuir* **26**, 943 (2010).
21 S. Selvanathan, M.V. Peters, J. Schwarz, S. Hecht and L. Grill, Applied Physics A **93**, 247 (2008).
22 J. Iwicki, E. Ludwig, M. Kalläne, J. Buck, F. Köhler, R. Herges, L. Kipp and K. Rossnagel, *Appl. Phys. Lett*. **97**, 063112 (2010).
23 A.S. Kumar, T. Ye, T. Takami, B.-C. Yu, A.K. Flatt, J.M. Tour and P.S. Weiss, *Nano Lett*. **8**, 1644 (2008).
24 G. Pace, V. Ferri, Ch. Grave, M. Elbing, C. von Hänisch, M. Zharnikov, M. Mayor, M. Anita Rampi and P. Samori, *Proc. Natl. Acad. Sci. U. S. A*. **104**, 9937 (2007).
25 J. Henzl, M. Mehlhorn, H. Gawronski, K._H. Rieder and K. Morgenstern, *Angew. Chem. Int. Ed*. **45**, 603 (2006).
26 M.J. Comstock, D.A. Strubbe, L. Berbil-Bautista, N. Levy, J. Cho, D. Poulsen, J.M.J. Fréchet, S.G. Louie and M.F. Crommie, *Phys. Rev. Lett*. **104**, 178301 (2010).
27 J. Cho, L. Berbil-Bautista, N. Levy, D. Poulsen, J.M.J. Fréchet and M.F. Crommie, *J. Chem. Phys*. C **133**, 234707 (2010).
28 A. Kirakosian, M.J. Comstock, J. Cho and M. F. Crommie, *Phys. Rev. B* **71**, 113409 (2005).
29 Y. Wen, W. Yi, L. Meng, M. Feng, G. Jiang, W. Yuan, Y. Zhang, H. Gao, L. Jiang and Y. Song, *J. Phys. Chem. B* **109**, 14465 (2005).
30 M. Wolf, P. Tegeder, *Sur. Sci*. **603**, 1506 (2009).
31 Y. Wang, X. Ge, G. Schull, R. Berndt, H. Tang, C. Bornholdt, F. Koehler and R. Herges, *J. Am. Chem. Soc*. **132**, 1196 (2010).
32 N. Atodiresei, V. Caciuc, J.-H. Franke and S. Blügel, *Phys. Rev. B* **78**, 045411 (2008).
33 D.B. Dougherty, J. Lee and J.T. Yates, *J. Phys. Chem B* **110**, 11991 (2006).
34 A. Bilić, J.R. Reimers and N.S. Hush, *J. Phys. Chem B* **106**, 6740 (2002).
35 D. Mollenhauer, N. Gaston, E. Voloshina and B. Paulus, *J. Phys. Chem. C* **117**, 4470 (2013).
36 T.E. Jones, C. Zuo, P.W. Jagodzinski and M.E. Eberhart, *J. Chem. Phys C* **111**, 5493 (2007).
37 H. Lange, J. Maultzsch, W. Meng, D. Mollenhauer, B. Paulus, N. Peica, S. Schlecht and Ch. Thomsen, *Langmuir* **27**, 7258 (2011).
38 F. Tao, M.H. Qiao, Z. H. Wang and G. Q. Xu, *J. Phys. Chem B* **107**, 6384 (2003).
39 R. Coustel, S. Carniato, F. Rochet and N. Witkowski, *Phys. Rev. B* **85**, 035323 (2012).
40 Y. P. Zhang, S. Wang and G. Q. Xu, J. *Phys. Chem C* **115**, 2140 (2011).
41 E. McNellis, J. Meyer and K. Reuter, *Phys. Rev. B* **80**, 205414 (2009).
42 B.-Y. Choi, S.-J. Kahng, S. Kim, H. Kim, H. W. Kim, Y. J. Song, J. Ihm and Y. Kuk, *Phys. Rev. Lett.* **96**, 156106 (2006).
43 E. McNellis, J. Meyer, A. D. Baghi and K. Reuter, *Phys. Rev. B* **80**, 035414 (2009).
44 G. Mercurio, E.R. McNellis, S. Hagen, F. Leyssner, S. Soubatch, J. Meyer, M. Wolf, P. Tegeder, 45F.S. Tautz and K. Reuter, *Phys. Rev. Lett.* **104**, 036102 (2010).
46 J.P. Prates Ramalho, F. Illas, *Chem. Phys. Lett*. 501, 379 (2011).
47 Y. Wang and H.-P. Cheng, *Phys. Rev. B* **86**, 035444 (2012).
48 J. Henzl, P. Puschnig, C. Ambrosch-Draxl, A. Schaate, B. Ufer, P. Behrens and K. Morgenstern, *Phys. Rev. B* **85**, 035410 (2012)
49 M. Alemani, S. Selvanathan, F. Ample, M.V. Peters, K.-H. Rieder, F. Moresco, Ch. Joachim, S. Hecht and L. Grill, *J. Phys. Chem. C* **112**, 10509 (2008).
50 A. Safiei, J. Henzl and K. Morgenstern, *Phys. Rev. Lett*. **104**, 216102 (2010).
51 S. Grimme, *J. Comput. Chem*. **25**, 1463 (2004).
52 S. Grimme, *J. Comput. Chem*. **27**, 1787 (2006).
53 S. Grimme, J. Antony, T. Schwabe, and C. Mück-Lichtenfeld, *Org. Biomol. Chem*. **5**, 741 (2007).
54 S. Grimme, S. Ehrlich, L. Goerigk, *J. Comput. Chem*. 32,1456 (2011).
55 S. Grimme, J. Antony, S. Ehrlich, S. Krieg, *Chem. Phys*. 132, 154104 (2010).
56 G. Kresse and J. Hafner, *Phys. Rev. B* **47**, 558 (1993).
57 G. Kresse and J. Furthmüller, *Phys. Rev. B* **54**, 11169 (1996).
58 P. Perdew, K. Burke and M. Ernzerhof, *Phys. Rev. Lett*. **77**, 3865 (1996).
59 P. E. Blöchl, *Phys. Rev. B* **50**, 17953 (1994).
60 G. Kresse and D. Joubert, *Phys. Rev. B* **59**, 1758 (1999).
61 T. Björkman, A. Gulans, A.V. Krasheninnikov and R.M. Nieminem, *J. Phys.: Condens. Matter* 24, 424218 (2012).
62 R. F. W. Bader, *Chem. Rev*. **91**, 893 (1991).
63 G. Henkelman, A. Arnaldsson, and H. Jónsson, *Comput. Mater. Sci.* **36**, 354 (2006).
64 D. Loffreda, *Angew. Chem*. **118**, 6687 (2006).
65 C. Liu, S. Zhang, P. Wang, S. Huang, H. Tian, *Int. J. Hydrogen Energy* **38**, 8367 (2013).
66 M.J.S. Spencer, K. W.J. Wong, I. Yarovsky, *Materials Chemistry and Physics* **119**, 505 (2010).
67 B. Silvi and A. Savin, Nature **371**, 683 (1994).
68 A. Savin, H. J. Flad, J. Flad, H. Preuss, H. G. von Schnering, *Angew. Chem. Int. Ed. Engl.* **31,** 185 (1992).
69 M. Kohout, K., Pernal, F. R. Wagner, Y. Grin, *Theor. Chem. Acc.* **112,** 453 (2004).
70 A.D. Becke, K.E. Edgecombe, *J. Chem. Phys*. **92,** 5397 (1990).
71 N. Ooi, A. Rairkar, L. Lindsley, J.B. Adams*, J. Phys.: Condens. Matter* **18**, 97 (2006).
72 M. Berthe, A. Urbieta, L. Perdigão, B. Grandidier, D. Deresmes, C. Delerue, D. Stiévenard, R. Rurali, N. Lorente, L. Magaud and P. Ordejón, *Phys. Rev. Lett* **97**, 206801 (2006).
73 F. Tao, M. H. Qiao, Z.H. Wang and G.Q. Xu, *J. Phys. Chem. B* 107, 6384 (2003).

74 Y.P. Zhang, S. Wang, G.Q. Xu, *J. Phys. Chem C* 115, 2140 (2011).
75 S. Hong, Y. E. Cho, J.Y. Maeng, S. Kim, *J. Phys. Chem B* 108, 15229 (2004)